



## Study on properties of ultrafiltration membrane prepared by hydrolyzed polyacrylonitrile

Yuyang Guo, Hongchao Zhang, Xuesong Zhang, Xuemei Hu, Chaoran Wang, Yanan Yang\*

*Special Polymer Materials Laboratory, Changchun University of Technology, Changchun 130012, China, Tel. +13089411940; email: yangyanan@ccut.edu.cn (Y.N. Yang), Tel. +13074399098; emails: 13074399098@163.com (Y.Y. Guo), 865942943@qq.com (H.C. Zhang), 1637384424@qq.com (X.S. Zhang), 821704712@qq.com (X.M. Hu), 1448840802@qq.com (C.R. Wang)*

Received 29 February 2020; Accepted 14 July 2020

---

### ABSTRACT

Hydrophilic polyacrylonitrile (HPAN) ultrafiltration membranes were successfully prepared by the phase inversion method with hydrolysis modified polyacrylonitrile as the basic materials. The effect of hydrolysis time of polyacrylonitrile on the morphology and performance of the HPAN ultrafiltration membranes were investigated by the approaches of ultrafiltration experiments, porosity testing, scanning electron microscopy, attenuated total reflectance-Fourier-transform infrared spectroscopy, water contact goniometer angle and dynamic anti-contamination. The results showed that the hydrophilicity, pore connectivity, porosity and pure water flux of the membranes could be improved by increasing the hydrolysis time of polyacrylonitrile (PAN). However, the longer hydrolysis time will lead to degradation of PAN, resulting in a decrease of the retention rate and mechanical strength. Through comprehensive consideration, when the hydrolysis time was 2 h, the HPAN ultrafiltration membrane exhibited excellent water permeate flux and good anti-pollution ability almost without decreasing the retention and mechanical strength. Thus, the proper hydrolysis degree could improve the separation efficiency, prolong the life cycle and reduce the operational costs of the polyacrylonitrile membrane. In addition, the presence of carboxyl groups due to hydrolysis provides unlimited possibilities for further modification of HPAN membranes.

*Keywords:* Polyacrylonitrile membrane; Hydrolysis modified; High water flux; Anti-pollution

---

### 1. Introduction

The technology of the ultrafiltration (UF) membrane has a promising future in the field of water resource recovery and utilization [1,2]. It can be applied as an effective strategy of water treatment as a result of its low-priced, easy development, operation and environmental-friendliness [3,4]. However, the industrial application of the ultrafiltration membrane is still limited by the problems of the membrane fouling, which requires additional cleaning processes to weaken pollution and increase operating

costs [5,6]. Additionally, fouling accumulation on the outside and in the pore of the membrane will provide an advantageous living condition for microbial propagation, which will damage the structure, shorten the lifetime of the membrane and pollute the filtrate [7–9].

Hence, it is of great significance to minimize fouling in UF membranes. Usually, the anti-pollution performance of the membranes could be improved by furthering their hydrophilicity [10,11]. The ground on this, many modifications were carried out such as blending, copolymerization

---

\* Corresponding author.

and surface modification. Kim et al. [12] immobilized nisin and dopamine on the skin layer of polysulfone ultrafiltration membranes, which effectively built up the anti-pollution performance of the ultrafiltration membrane. Hwang et al. [13] adsorbed a layer of graphene oxide onto the polysulfone membranes. The research data revealed that the hydrophilicity and the water flux were obviously improved. What's more, the amount of absorbed bovine serum albumin (BSA) was significantly reduced. Garcia-Ivars et al. [14] took polyethylene glycol (PEG) and  $Al_2O_3$  as the hydrophilic additives to polyethersulfone ultrafiltration membranes. His research data proved that the ultrafiltration performance and mechanical performance of polyethersulfone ultrafiltration membranes were both improved. In the previous research of our research team, we tried to enhance the performance of the ultrafiltration membrane by introducing nano titanium dioxide, and successfully introduced titanium dioxide nanoparticles and titanium dioxide sol into the polysulfone ultrafiltration membrane. The research found that the ultrafiltration performance, anti-pollution and mechanical properties of the ultrafiltration membrane have been significantly improved. In particular, the interpenetrating network formed by titanium dioxide sol and polysulfone is more prominent in performance improvement [15–17].

Polyacrylonitrile (PAN) ultrafiltration membrane has been diffusely used in the traditional ultrafiltration membrane process as a result of its excellent chemical and thermal stability and solvent resistance [18,19]. However, as a kind of hydrophobic material, PAN is also affected by the problem of membrane fouling. In order to improve the applicability of PAN materials in ultrafiltration technology, different researches were conducted by researchers. Meng et al. [20] deposited the chitosan layer on the skin-layer of the PAN basement membrane. Although the method can efficaciously enhance the hydrophilicity of UF membranes, it leads to a decrease in pore size of the basement membrane and a loss of pure water flux. Nie et al. [21] attached PEG400 to the PAN-MAH membrane and observed a significant increase in water flux and a significant decrease in the adsorption of BSA. Although PEG-based materials can achieve the required modification, they are readily oxidized in most biochemically related solutions. Beril Melbiah et al. [22] added titanium dioxide nanoparticles to PAN casting solution. The research found that the anti-pollution capacity and hydrophilicity of the PAN membrane had been efficaciously enhanced. However, the research also revealed that the addition of nanoparticles caused a certain degree of blockage of the membrane pore and it had a negative effect on the water permeability of the membrane. After the summarization of many studies, it is obvious that the introduction of relevant functional groups on the polymer backbone can effectively improve the anti-pollution performance while maintaining good water flux. Asatekin et al. [23] applied the amphiphilic comb copolymer PAN-graft-polyethylene oxide PAN-g-PEO as additives for the manufacture of new PAN UF membranes. The research turned out to be that water flux had been greatly improved as well as the anti-pollution ability. Although this modification method effectively improves the performance of the membrane, it increases the cost of the UF membrane in practical

production and application. Thus, researchers are devoted to finding an economical and effective modification method.

As is known to us, the cyanogen groups on side chains of PAN can hydrolyze to form carboxyl groups under the alkaline condition [24,25], which improves the hydrophilicity of PAN and make it shown response to pH. So, making PAN membranes hydrolyzed to improve the fouling resistance and hydrophilicity of the membrane has been a research focus [26].

In previous studies, some researchers have hydrolyzed the PAN membrane and grafted other functional groups. Although this method has achieved the purpose of modification, the negative impact of the hydrolysis after membrane formation on the PAN film is fatal, so we consider trying to hydrolyze the PAN material first, and then use the hydrolyzed polyacrylonitrile (HPAN) to form the membrane. In our study, a series of hydrophilic UF membranes were prepared by using the HPAN as materials. We investigated the effect of hydrolysis time of PAN on membrane structure and properties and then found that the proper hydrolysis time of PAN could improve morphology and hydrophilicity, increase the permeability and anti-fouling performance of the membranes.

## 2. Materials and methods

### 2.1. Chemical materials

Polyacrylonitrile powder ( $M_n = 50,000$ ) was purchased from BASF, Germany. Polyvinylpyrrolidone ( $M_r = 10,000$ ), *N,N*-dimethylacetamide (DMAc), *N*-methyl-2-pyrrolidone (NMP), purchased from Tianjin Ghuangfu, China. Hydrochloric acid (HCl, 36%–38%) and sodium hydroxide were analytical grades of Beijing Chemical Reagent Company (China Chemical Reagent Company). Bovine serum albumin (BSA, 67 kDa) was obtained from Beijing Dingguo Biotechnology (China). Anhydrous ethanol was purchased from Chengdu Kelong, China. Distilled water was prepared at the Changchun University of Technology.

### 2.2. Preparation of hydrolyzed PAN (HPAN)

HPAN is prepared by the alkaline hydrolysis of PAN. Briefly speaking, taking HPAN-1 h for an example, the virgin PAN was hydrolyzed by continuing stirring 1 h in NaOH solution (1 mol/L) at 60°C [27]. HPAN powder was collected from the sodium hydroxide solution by suction filtration, and HPAN also is washed many times with distilled water until the pH of the filtrate is neutral. Then the HPAN powder was obtained after the final drying at 55°C for 6 h in a temperature-controlled dryer. The hydrolysis mechanism of PAN is shown in Fig. 1.

### 2.3. Characterization of hydrolyzed PAN

The chemical constitution of HPAN was characterized by Fourier-transform infrared spectroscopy (FTIR) using AVATAR-360. The spectrums were recorded over the wavelength range of 500–4,000  $cm^{-1}$  using KBr pellets. The acid-base titration method was used to determine the degree of hydrolysis of the PAN powder by using phenolphthalein as an indicator in this experiment. The degree of

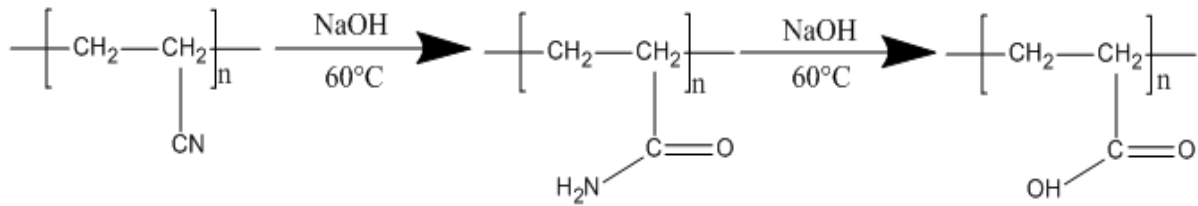


Fig. 1. Synthetic route of HPAN.

reaction (X) of the cyanogroup was calculated to according the following formula by testing the consumption of NaOH.

$$\frac{\frac{W_{\text{PAN}} \cdot X}{M_{\text{AN}}} \cdot W_{\text{O}}}{W_{\text{all}} - \frac{W_{\text{PAN}} \cdot M_{\text{NH}_3} \cdot X}{M_{\text{AN}}}} = \frac{\frac{M_{\text{NaOH}} \cdot W_{\text{O}}}{W_{\text{NaOH}}} - M_{\text{HCL}} \cdot V_{\text{HCL}} \cdot 10^{-3}}{W_{\text{all}} - \frac{W_{\text{PAN}} \cdot M_{\text{NH}_3} \cdot X}{M_{\text{AN}}}} \quad (1)$$

In the above formula,  $M_{\text{AN}}$ : molar mass of acrylonitrile structural unit,  $W_{\text{PAN}}$ : the total mass of PAN in reaction flask (g),  $M_{\text{NaOH}}$ : molecular weight of sodium hydroxide,  $W_{\text{NaOH}}$ : the total mass of NaOH in reaction flask (g),  $W_{\text{O}}$ : takeout titration reaction mass (g),  $W_{\text{all}}$ : the total mass of reactants in the reaction flask (g), including PAN, NaOH, water,  $M_{\text{NH}_3}$ : molar concentration of  $\text{NH}_3$ ,  $M_{\text{HCL}}$ : standard hydrochloric acid solution,  $V_{\text{HCL}}$ : standard hydrochloric acid consumed by titration volume (mL).

#### 2.4. Preparation of ultrafiltration membrane

The HPAN membranes were prepared via a non-solvent to induce the phase separation method (NIPs). HPAN powder (16 wt.%) with different hydrolysis time (0, 1, 2, 3, 4, and 6 h) and poly(vinylpyrrolidone) (4 wt.%) were dissolved in a mix solution of DMAc and NMP under the stirring condition for 12 h in order to make casting solution more homogeneous, and the casting solution has to be stored at room temperature for 24 h to remove air bubbles. Subsequently, the HPAN casting solution was poured onto a special plate and cast by a doctor blade (thickness: 0.18 mm) at room temperature, after about 15 s of solvent evaporation, the special plate with casting solution was quickly plunged into a coagulating bath to form a membrane by L-S phase inversion. The resulting HPAN membranes were placed in a distilled water bath at an indoor temperature and permitted to stand for 3 d to remove the remaining solvent and the HPAN membrane was kept in distilled water containing 1% formaldehyde to avoid bacterial growth [16,28]. The preparation flowchart is shown in Fig. 2.

#### 2.5. Morphological observation

The cross-section morphology of the HPAN membrane was observed by a JSM-6510 scanning electron microscopy (SEM, Japan Electron). The samples were fractured in liquid nitrogen and coated with a thin layer of gold before examined.

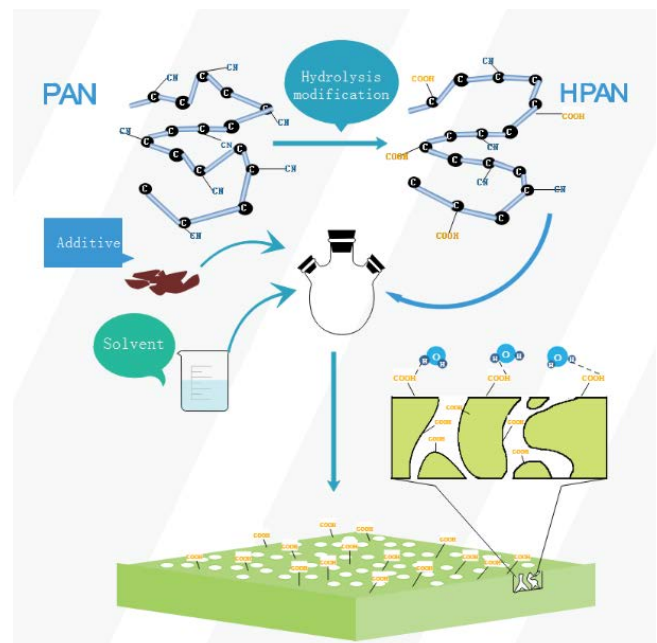


Fig. 2. Preparation flow chart of HPAN membrane.

#### 2.6. Ultrafiltration performances experiments

Ultrafiltration performances including the pure water flux and the retention of the HPAN membranes. In this study, the pure water flux was tested using the SCM300 ultrafiltration cup (Ecologic Center Shanghai) at room temperature. Each membrane in the cup was fed with distilled water for 15 min at 0.05 MPa before the test. The filtration time was 15 min, the volume of collecting water was recorded every 3 min during the filtration process and formed an average. The pure water permeability ( $J_w$ ) of the membranes were calculated by Eq. (2):

$$J_w = \frac{V}{A \times \Delta t} \quad (2)$$

In the formula,  $V$  (L) is the average volume of the filtrate;  $A$  ( $\text{m}^2$ ) is the filtration area;  $\Delta t$  (h) is the collection time.

In the ultrafiltration membrane retention performance experiment, we tested the ultrafiltration membrane's ability to retain bovine serum proteins (BSA, 67 kDa, Dingguo Biologic Tech). We still used the SCM300 ultrafiltration cup for testing. The BSA solution (0.1 g/L) was fed to the ultrafiltration cup for 15 min, with operating conditions were:

transmembrane pressure of 0.1 MPa, room temperature, and tangent speed of water is 3 m/s. The retention rate is calculated by Eq. (3):

$$R = \left( 1 - \frac{C_p}{C_0} \right) \times 100\% \quad (3)$$

where  $C_0$  is the concentration of BSA in the feed liquid,  $C_p$  the concentration of BSA in the filtrate, and the values of  $C_0$  and  $C_p$  are analyzed by an ultraviolet spectrophotometer (UV-1800) at 278.5 nm [29,30].

### 2.7. Hydrophilic test

In order to investigate the effect of alkaline modification of PAN on the hydrophilicity of ultrafiltration membranes, surface hydrophilicity was characterized by testing the water contact angle (WCA) with a Drop Shape Analyzer (DSA 100, Krüss GmbH, Hamburg, Germany). Before testing, all samples need to be washed to remove the loosely adsorbed substances on the membrane surface, and then dried in a 60°C vacuum oven for 24 h. For each sample, the contact angle was measured 5 times at different positions and then averaged.

### 2.8. Porosity and pore size test

Membrane porosity ( $\epsilon$ , %) was determined by the wet-dry gravimetric method. Before the test, a 6 cm × 6 cm membrane sample was washed to remove the materials adsorbed on the surface, and the weight of the wet membrane was weighed and recorded as  $W_1$ . Then the samples were dried in a blast drying oven at 55°C for 1 h and stayed in a vacuum dryer at 60°C for 24 h. The dry weight of the membrane at this time was weighed and recorded as  $W_2$ , and the porosity of the ultrafiltration membrane was calculated by Eq. (4):

$$\text{Porosity} = \frac{W_1 - W_2}{V \times \rho} \times 100\% \quad (4)$$

where  $V$  (cm<sup>3</sup>) is the volume of the membrane and  $\rho$  is the density of water at room temperature [15].

The pore size of the ultrafiltration membranes was tested by a capillary flow porometer (POROLUX500, Germany), and the pore size analysis was performed using computer software (POROLUX500, porometer). In this work, the POREFIL was used to wet membrane samples. Three measurements were performed on different batches of membranes made by the same method.

### 2.9. Mechanical strength tests

In this study, the mechanical strength of the HPAN membranes were measured on an INSTRON-3365 universal material testing machine. The membrane length was 30 mm and the loading speed was 3 mm/min. Each sample was tested three times in parallel.

### 2.10. Anti-pollution performance test

The antifouling property of the HPAN UF membrane was evaluated through a dynamic fouling experiment by using BSA as a model pollutant. The experiment was carried out at 0.1 MPa, a tangential water velocity of 3 m/s and room temperature with an SCM 300 ultrafiltration cup. First, the membrane was feed by distilled water at 0.1 MPa for 30 min to get steady-state flux registered as  $J_0$ , then was used to filtrate the BSA aqueous solution (1.0 g/L) as the fouling fluid until the flux stabilization. After that, the contaminated membrane in the ultrafiltration cup was flushed with distilled water for 20 min under the tangential velocity of about 3.0 m/s and the pressure of 0.05 MPa to clean all the unconsolidated BSA molecules deposited on the membrane surface. This process was repeated for 30 d and the final water flux was recorded as  $J_1$ . Observe the change of water flux with time and the recovery of water flux, expressed by the flux attenuation coefficient  $m$ :

$$m = \frac{J_0 - J_1}{J_1} \times 100\% \quad (5)$$

## 3. Results and discussion

### 3.1. Infrared spectra analysis for HPAN

We investigated the molecular structure changes of HPAN caused by different hydrolysis time through FTIR spectra (Fig. 3). In the infrared spectra of HPAN, we found that the absorption cyanogroup peaks of HPAN at 2,224 and 1,440 cm<sup>-1</sup> became weaker compared with PAN [31], and the absorption peak of carboxylate sodium groups appears at the position of 1,568 cm<sup>-1</sup>, which indicated that cyanogroups had hydrolyzed into carboxylic groups. In addition, the intensity of carboxyl absorption peaks at 1,568 cm<sup>-1</sup> became stronger with the hydrolysis time increasing. So, we can speculate that the content of carboxyl groups on the HPAN molecular chain increases with the increase of hydrolysis time.

### 3.2. Conversion rate of cynaogroup with different hydrolysis time

In this experiment, the conversion rate of cyanogen groups was tested through acid-base titration. The characterization results are shown in Fig. 4, the conversion rate of cyanogroups increased with the increase of hydrolysis time, especially at the initial stage of hydrolysis (about 1 h), the cyanogroup conversion rate increased rapidly, and then the increasing trend became gentle. This phenomenon may be related to the neighboring group effect of a macromolecule that when a part of cyanogroups are converted to carboxyl groups in the alkaline hydrolysis reaction of PAN, the hydrolysis of the adjacent cyanogroups will be limited because of the electrostatic repulsion of the carboxyl to OH-attack [24,32].

### 3.3. Analysis of membrane cross-section

The cross-section morphologies of PAN ultrafiltration membranes with different hydrolysis time were observed by SEM. As shown in Fig. 5, with the hydrolysis time of the

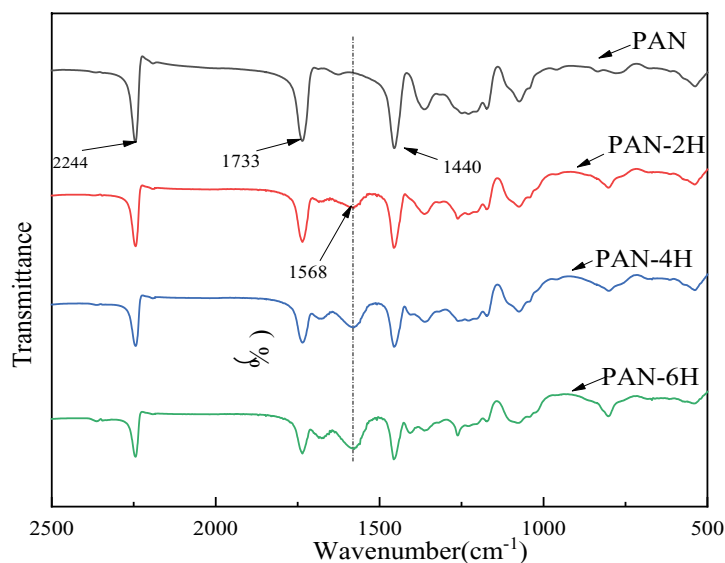


Fig. 3. Infrared spectra for HPAN with different hydrolysis time.

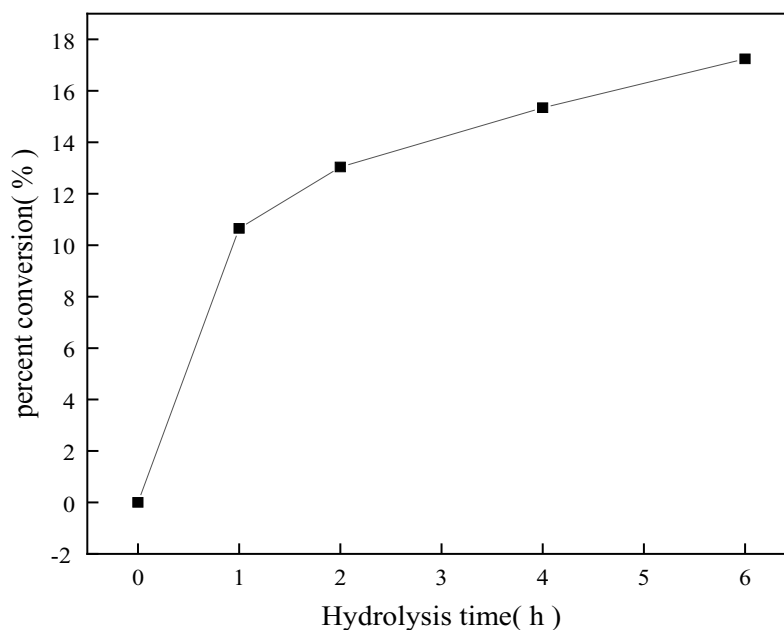


Fig. 4. Relationship between PAN cyanogroup conversion and hydrolysis time.

membrane material increasing, the sublayer structure of the membrane underwent a transition from the semi-finger-like pore to run-through finger-like pore structure, the volume of the finger pores increased and the thickness of the membrane skin layer became thinner (a, b, c, d, e). These variations of membrane structure could be explained that the hydrogen bond interaction between carboxyl groups formed through the PAN hydrolysis and water molecules accelerated the indiffusion rate of non-solvent to casting solution, which was the driving force to promote the growth of the macropores growth during the precipitation process

of wet-casting polymeric membranes, thereby causing the ultrafiltration membrane to produce a wider finger pore structure [15,16]. At the same time, the increase of the indiffusion rate of non-solvent to casting solution also induced a fast demixing process, preventing HPAN macromolecules to aggregate and rearrange to the membrane surface, resulting in the formation of a thinner skin layer.

However, the last image (f) showed that the cross-section of HPAN was damaged at longer hydrolysis time of PAN (6 h), which indicated that excessive hydrolysis led to the breaking of PAN molecular chains and then weaken the

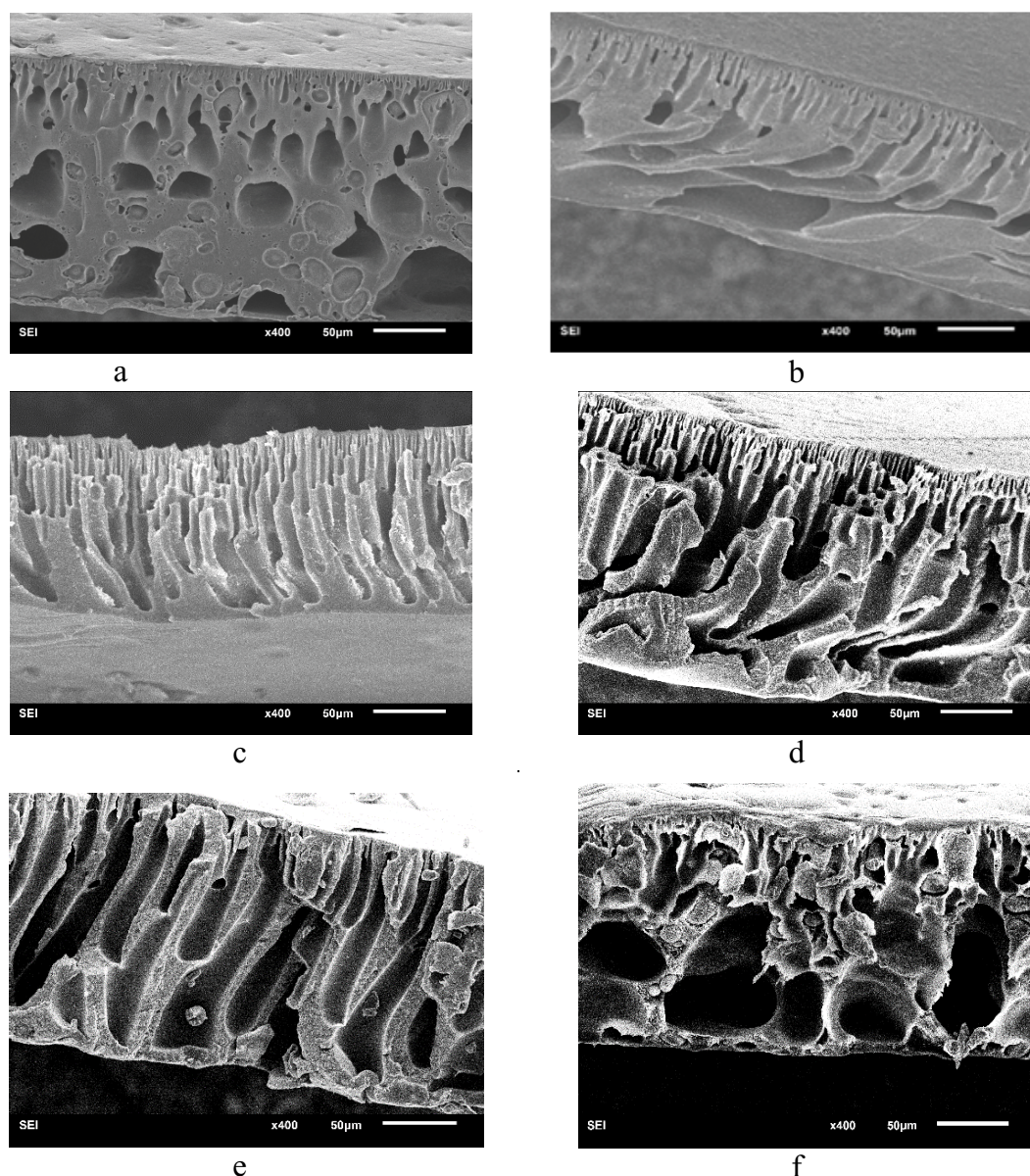


Fig. 5. SEM images of the cross-sections of the (a) PAN, (b) HPAN-1 h, (c) HPAN-2 h, (d) HPAN-3 h, (e) HPAN-4 h and (f) HPAN-6 h membrane.

film-forming property of HPAN. So, we can conclude that the hydrolysis time of PAN has a great influence on the membrane structure.

### 3.4. Hydrophilicity of membrane

The hydrophilicity of the ultrafiltration membrane is one of its main performances. The good hydrophilicity can be beneficial to increase the flux of membrane and improve the anti-pollution ability of ultrafiltration membranes. Generally, we characterize hydrophilicity by the water contact angle [33]. The better the hydrophilicity of the ultrafiltration membrane, the smaller the water contact angle. As shown in Fig. 6, the water contact angle of the HPAN membrane decreased gradually with the increase of hydrolysis time. It is

mainly because the carboxyl groups of the HPAN membrane could form hydrogen-bond with water molecules, which reduced the interfacial tension between water molecules and the membrane surface, thus decreasing the water contact angle, which resulted in the improvement of membrane hydrophilicity [34]. However, this decreasing tendency of the water contact angle began to slow down when the hydrolysis time was over 2 h, because the conversion rate of the cyanide group increased slowly with the increase of hydrolysis time, thus slowing down the increasing trend of carboxyl groups.

### 3.5. Porosity and pore size

As listed in Table 1, the porosity and the mean pore size of the membrane increased with the increase of hydrolysis

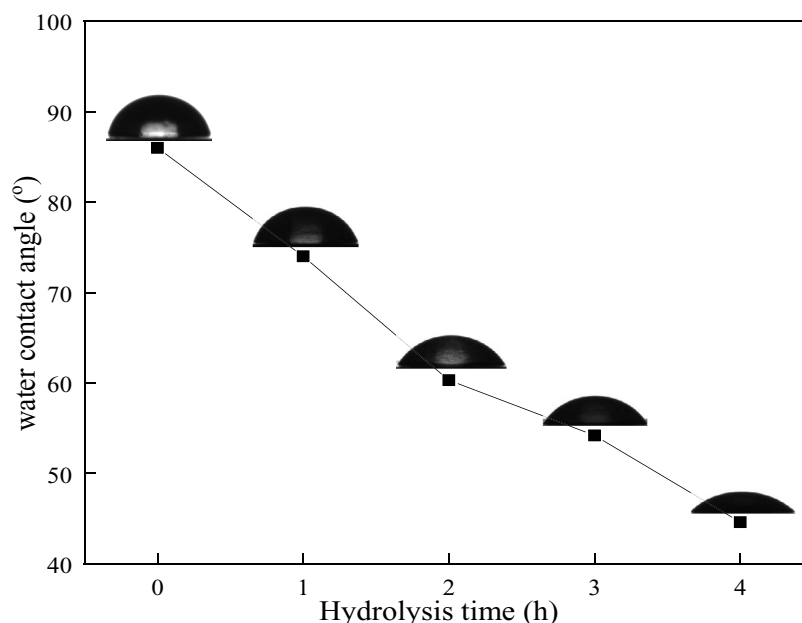


Fig. 6. The water contact angle of HPAN membrane with different hydrolysis time.

Table 1  
Average aperture of HPAN membranes with different hydrolysis time

PAN hydrolysis time (h)	Average aperture (nm)	Porosity (%)
0	31	69.3
1	38.5	75.6
2	49.4	80.38
3	80.4	83.37
4	91.2	85.24

time because of a fast L-S phase conversion process caused by the hydrogen-bonds between carboxyl groups of HPAN hydrolysis and water molecules, which prevented HPAN macromolecules to aggregate and rearrange fully to form a dense structure and resulted in a porous structure [16]. These findings are consistent with the SEM images (Fig. 5) and demonstrate that using HPAN as membrane material can increase its porosity and pore size. As a result, these pore structure changes can effectively improve the water flux of the ultrafiltration membrane.

### 3.6. Ultrafiltration performance

To investigate the influence of hydrolysis time on the pure water flux and BSA rejection rate of the membrane, the UF experiments were implemented. The results were shown in Fig. 7 indicated that with the increase of hydrolysis time, the pure water flux of membranes increased gradually, and the rejection rate decreased. These changes could be interpreted that during the filtration of the HPAN membrane, the carboxyl groups contained in HPAN improve the membrane hydrophilicity and attract water

molecules to pass through the membrane, the porosity became even larger and the big run-through finger-shaped pores were formed in the sublayer reduce the flow resistance of water, resulting in the increased of pure water flux [30]. While the decline of the BSA rejection rate is attributed to the thin skin layer and the macrovoids of the membrane [17,29], helping water molecules pass through the membrane and reducing membrane rejection gradually. When PAN was hydrolyzed for 2 h, the pure water flux of the membrane increased from 200 to 583 L/h m<sup>2</sup>, and the retention rate remained about 93% with little decline compared to the PAN membrane. Thus, according to the change of flux and rejection rate with hydrolysis time, we think the best hydrolysis time is 2 h when the HPAN membrane possesses superior UF performance.

### 3.7. Mechanical properties of membranes

The mechanical strength of HPAN ultrafiltration membranes was studied, and the relationship between tensile strength and elongation rate at the break of different HPAN membranes is illustrated in Fig. 8. The mechanical strength of the membranes decreased with the increase of hydrolysis time. This phenomenon is due to the hydrolysis of PAN, inducing the decline of PAN crystallinity and the more porous structure of membranes such as high porosity, macrovoids and run-through finger-like pores, which have a negative effect on the mechanical strengths of the membrane. Therefore, it is necessary to control the hydrolysis time of PAN in order to maintain the proper mechanical strength of membranes. When hydrolysis time is 2 h, although the tensile strength of the HPAN membrane decreases slightly (11.9%) compared with PAN, HPAN membranes possess superior UF performance and hydrophilicity, which are beneficial to improve the anti-pollution ability and operating efficiency of the membrane.

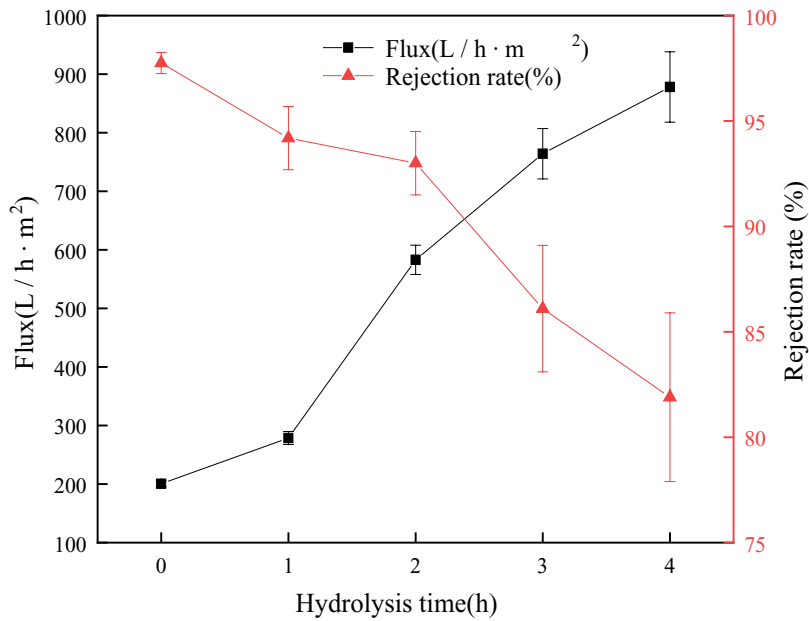


Fig. 7. Pure water flux and BSA rejection rate of HPAN membranes with different hydrolysis time.

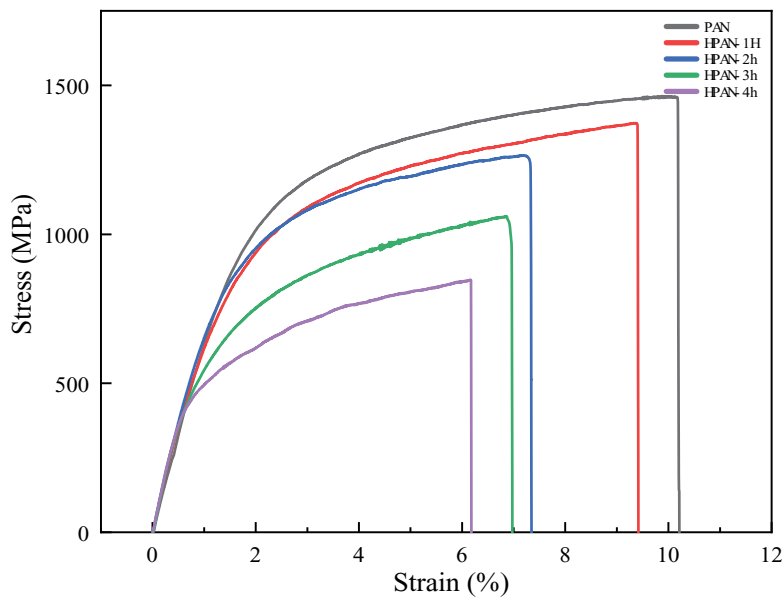


Fig. 8. Stress–strain curves of PAN and HPAN membranes.

### 3.8. Fouling resistance performance

The improved hydrophilicity of the membrane material could reduce contact and non-directional bonding between the membrane and contaminants, thereby reducing the adsorption of contaminants and facilitating the backwashing of the membrane [35]. In this work, we investigated the antifouling capability of the PAN membrane and the HPAN membrane with different hydrolysis time. The results are shown in Table 2, under the same operating conditions, the flux attenuation coefficient of the HPAN membranes decreases with the increase of the hydrolysis time, and the

flux attenuation caused by irreversible pollution is significantly reduced. This indicates that the improvement of the hydrophilicity of the membrane reduces the possibility of contact and the various bonding between and the membrane and the BSA, reducing the interaction between the membrane and the BSA, thereby weakening the adsorption and aggregation which caused membrane fouling [36–38]. In addition, since the carboxyl group carries the same negative charge as BSA, the repulsive force between them will also lead to a decrease in the adsorption capacity of hydrophobic solutes on the surface of the membrane, which will reduce the membrane pollution, and make the hydrophobic

Table 2  
Attenuated coefficient of water flux of membranes

	Initial water flux, $J_0$ (L/h m <sup>2</sup> )	Water flux after 30 d, $J_1$ (L/h m <sup>2</sup> )	Attenuated coefficient m
PAN	200	113	0.77
HPAN-1 h	273	207	0.32
HPAN-2 h	539	453	0.189
HPAN-3 h	731	660	0.10

solutes more easily fall off the membrane to reduce the flux attenuation during the backwash. Besides, as the carboxyl groups of HPAN carried the same negative charges as BSA molecules, the repulsive force between these two also attributed to the reduction of protein adsorption on the membrane surface [29], resulting in a reduction of membrane fouling and the hydrophobic solute is more easily detached during the backwashing process to reduce flux attenuation.

#### 4. Conclusion

In this study, a type of hydrophilic ultrafiltration membrane was prepared via phase inversion method by using the hydrolyzed polyacrylonitrile as membrane material. The effects of PAN hydrolysis time on the structure and performances of the membrane were investigated. With the increase of hydrolysis time of PAN, the porosity and size of the pore of PAN membranes increased. The hydrophilicity, pure water flux and anti-pollution ability of PAN membranes improved significantly, but the retention rate and mechanical strength decreased slightly. When the hydrolysis time lasted for 2 h, the retention rate and mechanical strength decreased 4% and 11.9% respectively. However, the pure water flux of the HPAN membrane can reach 2.9 times that of the PAN membrane, the water contact angle was reduced by 41.4°, the porosity reached 80%, and the flux attenuation coefficient was reduced by 0.58 from 0.77 of PAN membrane, showing excellent Anti-pollution performance. Therefore, the preparation of ultrafiltration membranes using PAN with appropriate hydrolysis could significantly improve the performance of the membrane, enhancing the fouling resistance and lifetime of the membrane. In the next research, we will try to further functionalize the HPAN ultrafiltration with a more active carboxyl reaction point.

#### References

- [1] A. Cassano, A. Basile, Chapter 20 – Membranes for Industrial Microfiltration and Ultrafiltration, A. Basile, S.P. Nunes, Eds., Advanced Membrane Science and Technology for Sustainable Energy and Environmental Applications, Woodhead Publishing Series in Energy, Cambridge, UK, 2011, pp. 647–679.
- [2] V. Calabrò, A. Basile, Chapter 1 – Fundamental Membrane Processes, Science and Engineering, A. Basile, S.P. Nunes, Eds., Advanced Membrane Science and Technology for Sustainable Energy and Environmental Applications, Woodhead Publishing Series in Energy, Cambridge, UK, 2011, pp. 3–21.
- [3] D.M. Warsinger, S. Chakraborty, E.W. Tow, M.H. Plumlee, C. Bellona, S. Loutatidou, L. Karimi, A.M. Mikelonis, A. Achilli, A. Ghassemi, L.P. Padhye, S.A. Snyder, S. Curcio, C.D. Vecitis, H.A. Arafat, J.H. Lienhard V, A review of polymeric membranes and processes for potable water reuse, *Prog. Polym. Sci.*, 81 (2016) 209–237.
- [4] W. Gao, H. Liang, J. Ma, M. Han, Z.-l. Chen, Z.-s. Han, G.-b. Li, Membrane fouling control in ultrafiltration technology for drinking water production: a review, *Desalination*, 272 (2011) 1–8.
- [5] A. Khan, T.A. Sherazi, Y. Khan, S. Li, S.A.R. Naqvi, Z. Cui, Fabrication and characterization of polysulfone/modified nanocarbon black composite antifouling ultrafiltration membranes, *J. Membr. Sci.*, 554 (2018) 71–82.
- [6] Z. Xu, J. Liao, H. Tang, N. Li, Antifouling polysulfone ultrafiltration membranes with pendent sulfonamide groups, *J. Membr. Sci.*, 548 (2018) 481–489.
- [7] A. Aguiar, L. Andrade, L. Grossi, W. Pires, M. Amaral, Acid mine drainage treatment by nanofiltration: a study of membrane fouling, chemical cleaning, and membrane ageing, *Sep. Purif. Technol.*, 192 (2018) 185–195.
- [8] X. Shi, G. Tal, N.P. Hankins, V. Gitis, Fouling and cleaning of ultrafiltration membranes: a review, *J. Water Process Eng.*, 1 (2014) 121–138.
- [9] W. Guo, H.H. Ngo, J. Li, A mini-review on membrane fouling, *Bioresour. Technol.*, 122 (2012) 27–34.
- [10] P.S. Goh, W.J. Lau, M.H.D. Othman, A.F. Ismail, Membrane fouling in desalination and its mitigation strategies, *Desalination*, 425 (2018) 130–155.
- [11] H.G. Sun, X.B. Yang, Y.Q. Zhang, X.Q. Cheng, Y.C. Xu, Y.P. Bai, L. Shao, Segregation-induced in situ hydrophilic modification of poly(vinylidene fluoride) ultrafiltration membranes via sticky poly(ethylene glycol) blending, *J. Membr. Sci.*, 563 (2018) 22–30.
- [12] J.-j. Kim, K. Kim, Y.-S. Choi, H. Kang, D.M. Kim, J.-C. Lee, Polysulfone based ultrafiltration membranes with dopamine and nisin moieties showing antifouling and antimicrobial properties, *Sep. Purif. Technol.*, 202 (2018) 9–20.
- [13] T. Hwang, J.-S. Oh, W. Yim, J.-D. Nam, C. Bae, H.-i. Kim, K.J. Kim, Ultrafiltration using graphene oxide surface-embedded polysulfone membranes, *Sep. Purif. Technol.*, 166 (2016) 41–47.
- [14] J. Garcia-Ivars, M.-I. Alcaina-Miranda, M.-I. Iborra-Clar, J.-A. Mendoza-Roca, L. Pastor-Alcañiz, Enhancement in hydrophilicity of different polymer phase-inversion ultrafiltration membranes by introducing PEG/Al<sub>2</sub>O<sub>3</sub> nanoparticles, *Sep. Purif. Technol.*, 128 (2014) 45–57.
- [15] Y. Yang, P. Wang, Preparation and characterizations of a new PS/TiO<sub>2</sub> hybrid membranes by sol-gel process, *Polymer*, 47 (2006) 2683–2688.
- [16] Y. Yang, P. Wang, Q.Z. Zheng, Preparation and properties of polysulfone/TiO<sub>2</sub> composite ultrafiltration membranes, *J. Polym. Sci., Part B: Polym. Phys.*, 44 (2006) 879–887.
- [17] Y. Yang, H.X. Zhang, P. Wang, Q.Z. Zheng, J. Li, The influence of nano-sized TiO<sub>2</sub> fillers on the morphologies and properties of PSF UF membrane, *J. Membr. Sci.*, 288 (2007) 231–238.
- [18] Y.B. Peng, F. Guo, Q.Y. Wen, F. Yang, Z.G. Guo, A novel polyacrylonitrile membrane with a high flux for emulsified oil/water separation, *Sep. Purif. Technol.*, 184 (2017) 72–78.
- [19] W. Zhao, L. Liu, L. Wang, N. Li, Functionalization of polyacrylonitrile with tetrazole groups for ultrafiltration membranes, *RSC Adv.*, 6 (2016) 72133–72140.
- [20] H. Meng, Q. Cheng, H.Z. Wang, C.X. Li, Improving anti-protein-fouling property of polyacrylonitrile ultrafiltration membrane by grafting sulfobetaine zwitterions, *J. Chem.*, 2014 (2014) 1–9.
- [21] F.-Q. Nie, Z.-K. Xu, Q. Yang, J. Wu, L.-S. Wan, Surface modification of poly(acrylonitrile-co-maleic acid) membranes by the immobilization of poly(ethylene glycol), *J. Membr. Sci.*, 235 (2004) 147–155.
- [22] J.S. Beril Melbiah, J. Pramila, D. Rana, A. Nagendran, N. Nagendra Gandhi, D. Mohan, Customized antifouling polyacrylonitrile ultrafiltration membranes for effective removal of organic contaminants from aqueous stream, *J. Chem. Technol. Biotechnol.*, 94 (2018) 859–868.
- [23] A. Asatekin, S. Kang, M. Elimelech, A.M. Mayes, Anti-fouling ultrafiltration membranes containing polyacrylonitrile-graft-poly(ethylene oxide) comb copolymer additives, *J. Membr. Sci.*, 298 (2007) 136–146.

- [24] A.D. Litmanovich, N.A. Plate, Alkaline hydrolysis of polyacrylonitrile, On the reaction mechanism, *Macromol. Chem. Phys.*, 201 (2000) 2176–2180.
- [25] P. Bhunia, S. Chatterjee, P. Rudra, S. De, Chelating polyacrylonitrile beads for removal of lead and cadmium from wastewater, *Sep. Purif. Technol.*, 193 (2018) 202–213.
- [26] Y. Hu, Z. Lü, C. Wei, S. Yu, M. Liu, C. Gao, Separation and antifouling properties of hydrolyzed PAN hybrid membranes prepared via *in-situ* sol-gel SiO<sub>2</sub> nanoparticles growth, *J. Membr. Sci.*, 545 (2018) 250–258.
- [27] D. Lunhan, Y. Liangju, Z. Dechun, Study on hydrolysis of polyacrylonitrile waste, *Anhui Chem. Ind.*, 3 (1994) 31–37.
- [28] Z.X. Liu, Z.M. Mi, C.H. Chen, H.W. Zhou, X.G. Zhao, D.M. Wang, Preparation of hydrophilic and antifouling polysulfone ultrafiltration membrane derived from phenolphthalin by copolymerization method, *Appl. Surf. Sci.*, 401 (2017) 69–78.
- [29] D. Zhou, G.L. Rong, S. Huang, J.H. Pang, Preparation of a novel sulfonated polyphenylene sulfone with flexible side chain for ultrafiltration membrane application, *Sep. Purif. Technol.*, 210 (2019) 817–823.
- [30] J.L. Shen, Q. Zhang, Q. Yin, Z.L. Cui, W.X. Li, W.H. Xing, Fabrication and characterization of amphiphilic PVDF copolymer ultrafiltration membrane with high anti-fouling property, *J. Membr. Sci.*, 521 (2017) 95–103.
- [31] H.F.M. Austria, R.L.G. Lecaros, W.-S. Hung, L.L. Tayo, C.-C. Hu, H.-A. Tsai, K.-R. Lee, J.-Y. Lai, Investigation of salt penetration mechanism in hydrolyzed polyacrylonitrile asymmetric membranes for pervaporation desalination, *Desalination*, 463 (2019) 32–39.
- [32] V. Igor, A.I.R. Ermakov, D. Arkady, A. Litmanovich, A. Nicolai, Plate alkaline hydrolysis of polyacrylonitrile, 1 structure of the reaction products, *Macromol. Chem. Phys.*, 201 (2000) 1415–1418.
- [33] H.T. Huang, J. Yu, H.X. Guo, Y. Shen, F. Yang, H. Wang, R. Liu, Y. Liu, Improved antifouling performance of ultrafiltration membrane via preparing novel zwitterionic polyimide, *Appl. Surf. Sci.*, 427 (2018) 38–47.
- [34] M. Yong, Y.Q. Zhang, S. Sun, W. Liu, Properties of polyvinyl chloride (PVC) ultrafiltration membrane improved by lignin: hydrophilicity and antifouling, *J. Membr. Sci.*, 575 (2019) 50–59.
- [35] Z.-W. Dai, L.-S. Wan, Z.-K. Xu, Surface glycosylation of polyacrylonitrile ultrafiltration membrane to improve its anti-fouling performance, *J. Membr. Sci.*, 325 (2008) 479–485.
- [36] H. Meng, Q. Cheng, C.X. Li, Polyacrylonitrile-based zwitterionic ultrafiltration membrane with improved anti-protein-fouling capacity, *Appl. Surf. Sci.*, 303 (2014) 399–405.
- [37] Q. Sun, Y.L. Su, X.L. Ma, Y.Q. Wang, Z.Y. Jiang, Improved antifouling property of zwitterionic ultrafiltration membrane composed of acrylonitrile and sulfobetaine copolymer, *J. Membr. Sci.*, 285 (2006) 299–305.
- [38] X.Y. Guo, S.G. Fan, Y.D. Hu, X.L. Fu, H.Q. Shao, Q.X. Zhou, A novel membrane biofouling mitigation strategy of D-amino acid supported by polydopamine and halloysite nanotube, *J. Membr. Sci.*, 579 (2019) 131–140.